

Superconducting critical temperature and dimensionality tuning of RbV_3Sb_5 via biaxial strain

Tsz Fung Poon^{§,1} King Yau Yip^{§,1} Ying Kit Tsui,^{1,2} Lingfei Wang,¹ Kai Ham Yu,¹ Wei Zhang,¹ Zheyu Wang,¹ Taketo Nakatani,³ Chishiro Michioka,³ Hiroaki Ueda,⁴ Siu Tung Lam,¹ Kwing To Lai,^{1,5} and Swee K. Goh^{*1}

¹*Department of Physics, The Chinese University of Hong Kong, Shatin, Hong Kong, China*

²*Quantum Science Center of Guangdong-Hong Kong-Macao Greater Bay Area, Shenzhen, China*

³*Division of Chemistry, Graduate School of Science, Kyoto University, Kyoto, Japan*

⁴*Co-Creation Institute for Advanced Materials, Shimane University, Matsue, Japan*

⁵*Shenzhen Research Institute, The Chinese University of Hong Kong, Shatin, Hong Kong, China*

(*skgoh@cuhk.edu.hk)

(Dated: 23 June 2025)

Kagome metal AV_3Sb_5 ($\text{A}=\text{K}, \text{Rb}, \text{Cs}$) has emerged as an intriguing platform for exploring the interplay between superconductivity and other quantum states. Among the three compounds, RbV_3Sb_5 has a notably lower superconducting critical temperature (T_c) at ambient pressure, posing challenges in exploring the superconducting state. For instance, the upper critical field (H_{c2}) is small and thus difficult to measure accurately against other control parameters. Hence, enhancing superconductivity would facilitate H_{c2} measurements, providing insights into key superconducting properties such as the dimensionality. In this letter, we report the tuning of the T_c in RbV_3Sb_5 through the application of biaxial strain. Utilizing a negative thermal expansion material ZrW_2O_8 as a substrate, we achieve a substantial biaxial strain of $\varepsilon = 1.50\%$, resulting in a remarkable 75% enhancement in T_c . We investigate the H_{c2} as a function of temperature, revealing a transition from multi-band to single-band superconductivity with increasing tensile strain. Additionally, we study the H_{c2} as a function of field angle, revealing a plausible correlation between the T_c enhancement and the change in dimensionality of the superconductivity under tensile strain. Further analysis quantitatively illustrates a transition towards two-dimensional superconductivity in RbV_3Sb_5 when subjected to tensile strain. Our work demonstrates that the application of biaxial strain allows for the tuning of both the T_c and superconducting dimensionality in RbV_3Sb_5 .

The quest for enhanced superconductivity remains one of the foremost endeavors in the field of condensed matter physics. When a superconductor has a low critical temperature (T_c), the associated critical magnetic fields are typically small, hindering the examination of the superconducting state through the measurement of the critical fields. Efforts to tune T_c include the application of hydrostatic pressure, which shrinks the crystal volume isotropically and modifies both the electronic band structure and the phonon spectrum. Successful examples of a significant increase in T_c by hydrostatic pressure include iron-based^{1–5} and cuprate^{6–9} superconductors. Superconductors with reduced crystal dimensionality, such as two-dimensional (2D) or quasi-2D compounds, have been heavily studied in recent years. The ability to tune the superconductivity of these systems is similarly important. Analogous to the case of tuning three-dimensional bulk superconductors, biaxial strain, which can vary the crystal area isotropically, emerges as a promising tuning tool for studying 2D superconductors.

A simple biaxial device can be assembled by mechanically bonding the superconductor to a substrate with different thermal expansion coefficients. Due to this thermal expansion mismatch between the sample and the substrate, a biaxial strain develops in-plane during cooling and reaches saturation at the zero-temperature limit. This novel technique has been utilized for the studies of superconductivity in various materials, such as those reported in Refs. [10–13]. Given the simplicity of the setup, it can be conveniently accommodated

in various sample spaces. For example, the biaxial device can be rotated in most laboratory magnets, enabling the measurement of the upper critical field (H_{c2}) as a function of the field angle.

Recently, the kagome metal AV_3Sb_5 ($\text{A}=\text{K}, \text{Rb}, \text{Cs}$)^{14,15} has emerged as an intriguing platform for exploring the interplay among its various quantum states. This is because the kagome lattice intrinsically hosts flat bands, van Hove singularities, and Dirac points in the electronic structure^{14–19}. Within the three members in the AV_3Sb_5 family, CsV_3Sb_5 is the most heavily studied, arguably because it has the highest T_c (~ 2.7 K) at ambient pressure^{20–28}. The lower T_c members, KV_3Sb_5 ^{29–35} and RbV_3Sb_5 ^{34–39}, deserve more experimental attention. Thus, it is desirable to increase their T_c systematically.

In this manuscript, we apply the biaxial strain tuning methodology to investigate RbV_3Sb_5 . We first report the superconducting transition in RbV_3Sb_5 coupled to different substrates. For the device with the enhanced T_c , we further measure H_{c2} against the temperature as well as the field angle. Our data allow us to identify the driving force behind the T_c enhancement, and discuss the dimensionality of the superconductivity. We also demonstrate how a large tensile strain can be achieved, by resorting to a negative thermal expansion material (ZrW_2O_8)⁴⁰. Our results showcase the versatility of the biaxial strain method and pave the way to the understanding of the superconductivity in the AV_3Sb_5 family.

High-quality single crystals of RbV_3Sb_5 were synthesized

by the self-flux method as described in Ref. [36]. Single crystals from the same batch were cleaved and cut into small strips of typical dimensions $800 \times 250 \times 10 \mu\text{m}^3$ for measurements under biaxial strain ϵ . The ZrW_2O_8 substrates were prepared from ZrO_2 (Nacalai Tesque, 98%) and WO_3 (Nacalai Tesque, 99.5%) powders. These powders were mixed stoichiometrically, pressed into pellets, and heated for 12 hours at 1200°C , the temperature determined based on the phase diagram given by Ref. [41]. The pellets were then quenched in liquid nitrogen to prevent decomposition into ZrO_2 and WO_3 . The pellets were subsequently ground, pressed into thin disks, heated, and quenched again. X-ray diffraction data, presented in Supplementary Material, confirms the formation of ZrW_2O_8 . Biaxial strain can be induced on the sample by the difference in thermal expansion between the sample and the substrate. The small size of the sample ensures that strain is effectively imposed on the sample by the substrate. Compressive strain ($\epsilon < 0$) was induced by attaching RbV_3Sb_5 to polycarbonate substrates with Cyanoacrylate (CN) adhesives. Similarly, different magnitudes of the tensile strain ($\epsilon > 0$) were induced by attaching RbV_3Sb_5 to cover glass, sapphire, diamond, and ZrW_2O_8 substrates with ThreeBond 2086M two-component epoxy resin adhesive (ThreeBond Holdings Co., Ltd.). In the process of attaching the samples to these substrates, the substrates were slightly heated for the better flow of the adhesive. The strain of sample and that of substrate were characterized by strain gauges (Tokyo Measuring Instruments Lab Co., Ltd.). The resultant strain induced on the sample at zero-temperature limit can be calculated as described in Ref. [13]. See the Supplementary Material for more details. A standard four-probe method was used to measure electrical resistance. A Bluefors dilution refrigerator provides the low-temperature environment down to 10 mK. A superconducting vector magnet was adopted for applying a vector field of 3 T/5 T (y/z-axes) to study the angular dependence of the upper critical field.

Figure 1(a) shows the normalized temperature dependence of electrical resistance around the superconducting transition for RbV_3Sb_5 experiencing different strains. For the free-standing sample ($\epsilon = 0$), T_c is 0.83 K. Here, T_c is defined as the temperature at which the resistance drops to 10% of the normal state value. Under compressive strain, T_c decreases to 0.61 K. Thus, in an attempt to increase T_c , we look for materials with a thermal expansion coefficient smaller than that of RbV_3Sb_5 to induce a tensile strain in the sample. For example, diamond is known to have a negligible thermal expansion coefficient: at 4 K, the lattice parameter a only decreases by $3 \times 10^{-4} \text{ \AA}$ from the room temperature value of 3.5671 \AA ⁴³. As shown in Fig. 1(a), T_c of RbV_3Sb_5 placed on diamond is enhanced to 1.30 K. Enhancement in T_c has also been observed when sapphire and cover glass were used. To create an even larger tensile strain, we turned to ZrW_2O_8 , which is a material with a negative thermal expansion⁴⁰. The usage of ZrW_2O_8 substrate allows us to achieve a large tensile strain of $\epsilon = 1.50\%$. Correspondingly, T_c is enhanced to a value as large as 1.46 K.

Figure 1(b) shows the percentage change in T_c ($\Delta T_c/T_c$) extracted from our result for RbV_3Sb_5 (filled circles) and that

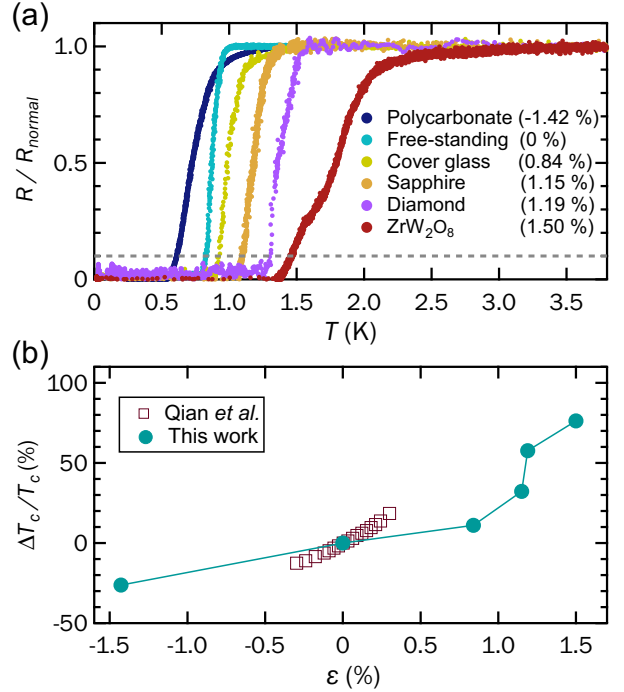


FIG. 1. (a) Temperature dependence of normalized resistance curves, showing the superconducting transitions of RbV_3Sb_5 with different substrates. The calculated strain induced in the low-temperature limit is shown in the brackets. The horizontal gray dashed line indicates the 10% criterion for the definition of T_c . (b) Percentage change of superconducting temperature $\Delta T_c/T_c$ as the function of strain summarized from (a), the square marker represents the $\epsilon_{A_{1g}}$ component extracted from the uniaxial strain study on CsV_3Sb_5 from Qian *et al.*⁴².

from Ref. [42] for CsV_3Sb_5 (open squares). Here, $\Delta T_c/T_c$ is defined as $[T_c(\epsilon) - T_c(\epsilon = 0)]/T_c(\epsilon = 0)$. For a valid comparison, we extract the biaxial component from the uniaxial strain experiment described in Ref. [42]. Specifically, we are interested in the isotropic response $\epsilon_{A_{1g}}$ of the uniaxial strain experiment, as described in Supplementary Material. For RbV_3Sb_5 , $\Delta T_c/T_c$ increases approximately linearly as ϵ increases from -1.42% to 0.84% . This is followed by an upturn when ϵ exceeds 0.84% , with $\Delta T_c/T_c$ reaching 75% when $\epsilon = 1.50\%$. On the other hand, $\Delta T_c/T_c$ as the function of (biaxial) strain in CsV_3Sb_5 is dominated by the linear term without slope changing. Overall, the use of substrates with progressively smaller, and even negative, thermal expansion allowed us to exert large tensile strain on RbV_3Sb_5 , revealing a surprising upturn in $\Delta T_c/T_c$. It would be interesting to explore if the upturn can be detected in CsV_3Sb_5 with a larger tensile strain. Typically, due to the Poisson effect, when a tensile biaxial strain is applied in the ab -plane, a compressive strain is induced along the c -axis. Similarly, when a tensile uniaxial strain is applied along an in-plane axis, a compressive strain is induced along the orthogonal in-plane axis and the c -axis. In Ref. [42], the strain along the c -axis is argued to be the dominant driving factor for T_c enhancement. This viewpoint is further supported by other strain studies on CsV_3Sb_5 ^{44,45}. Since both RbV_3Sb_5

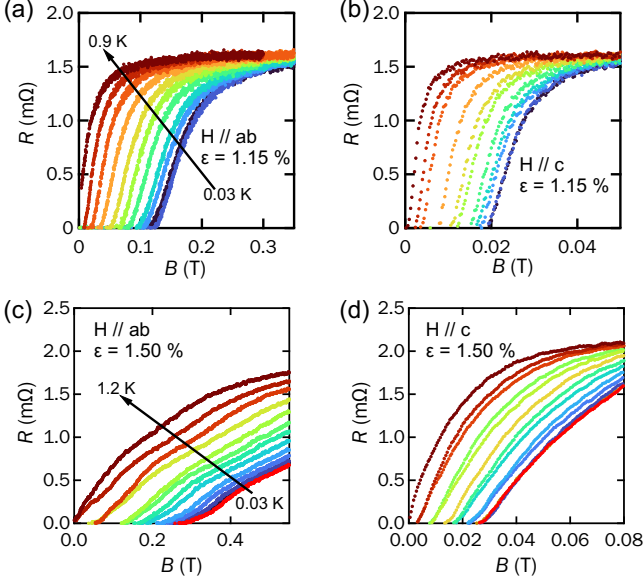


FIG. 2. Field dependence of the electrical resistance in RbV_3Sb_5 under tensile strain at different temperatures, for (a) $\varepsilon = 1.15\%$ and $H \parallel ab$, (b) $\varepsilon = 1.15\%$ and $H \parallel c$, (c) $\varepsilon = 1.50\%$ and $H \parallel ab$, and (d) $\varepsilon = 1.50\%$ and $H \parallel c$.

and CsV_3Sb_5 respond to strain in a similar manner, as suggested by the similar trend of T_c enhancement, the underlying tuning parameter of T_c for RbV_3Sb_5 is also the strain along the c -axis, and the strain in the ab -plane only plays a marginal effect. All in all, the strain along the c -axis appears to be the main driving force in T_c enhancement in RbV_3Sb_5 and CsV_3Sb_5 .

The largely enhanced T_c in RbV_3Sb_5 under biaxial tensile strain facilitates the measurement of the field dependence of the electrical resistance for the extraction of the H_{c2} . Figures 2(a) and 2(b) show the field dependence of the resistance in RbV_3Sb_5 under tensile strain of $\varepsilon = 1.15\%$, with the applied field in the ab -plane ($H \parallel ab$) and along the c -axis ($H \parallel c$), respectively. Likewise, Figs. 2(c) and 2(d) show the field dependence of the resistance in RbV_3Sb_5 under the largest tensile strain of $\varepsilon = 1.50\%$ for the two field orientations. In all cases, the zero resistance persists to higher field as the temperature decreases. To understand the pair-breaking mechanism of Cooper pairs associated with the drastic enhancement in T_c of RbV_3Sb_5 under tensile strain, we examine the H_{c2} as a function of temperature.

Figures 3(c) and 3(d) show the temperature dependence of the H_{c2} in RbV_3Sb_5 under tensile strain of $\varepsilon = 1.15\%$ and $\varepsilon = 1.50\%$, respectively. Here, H_{c2} is defined as the magnetic field at which the resistance drops to 10% of that in the zero-field normal state, and the temperature axis is expressed in the reduced unit, namely $t = T/T_c$. For $\varepsilon = 1.15\%$, $H_{c2}(t)$ shows trace of an upturn (indicated by the black arrow in Fig. 3(c)) near $t = 1$ for $H \parallel ab$. Such an upturn feature has also been reported for CsV_3Sb_5 , and it has been interpreted as a sign of multi-band superconductivity⁴⁶. Surprisingly, when the tensile strain increases to $\varepsilon = 1.50\%$, the upturn disap-

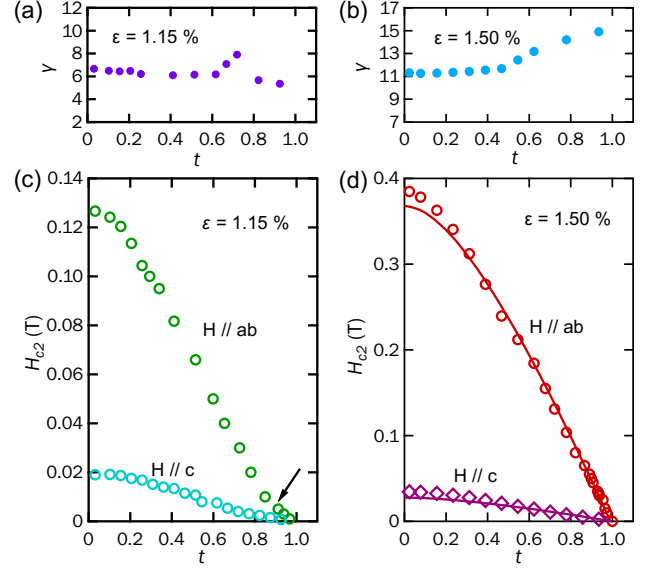


FIG. 3. Temperature dependence of upper critical field $H_{c2}(t)$ in RbV_3Sb_5 under tensile strain of (c) $\varepsilon = 1.15\%$ and (d) $\varepsilon = 1.50\%$, where $t = T/T_c$ is the reduced temperature. The solid lines in (d) represent the simulated $H_{c2}(t)$ by the WHH model. Temperature dependence of the extracted γ for (a) $\varepsilon = 1.15\%$ and (b) $\varepsilon = 1.50\%$.

pears, suggesting single-band superconductivity⁴⁷. In addition, the $H_{c2}(t)$ shows a linear dependence over a wide temperature range from $t = 1$. Therefore, we simulate the single-band Werthamer-Helfand-Hohenberg (WHH) model⁴⁷, with Maki parameter $\alpha = 0$ and the spin-orbit coupling $\lambda = 0$ for both field directions. The results of the simulations are represented by the solid lines, which are in good agreement with the experimental data (Fig. 3(d)). The orbital-limited field at zero temperature $H_{c2}^{orb}(0)$ can be obtained from the WHH simulations, and they are found to be 0.37 T and 0.03 T for $H \parallel ab$ and $H \parallel c$, respectively. Overall, the results imply that upon a moderate tensile strain ($\varepsilon = 1.15\%$), RbV_3Sb_5 exhibit the multi-band behavior, which is commonly shared in the AV_3Sb_5 family⁴⁶. By applying an unprecedentedly large tensile strain on RbV_3Sb_5 , we observed a single band behavior in $H_{c2}(t)$.

Next, we investigate the anisotropy factor γ , defined as $\gamma = H_{c2}^{||ab}/H_{c2}^{||c}$, where the superscript stands for the field direction. Figures 3(a) and (b) show the temperature dependence of γ for the tensile-strained RbV_3Sb_5 with $\varepsilon = 1.15\%$ and $\varepsilon = 1.50\%$, respectively. Comparing the two cases, with the larger tensile strain, γ is significantly larger for the whole temperature range. In particular, at 30 mK, γ is 6.7 for $\varepsilon = 1.15\%$ but it is significantly enhanced to 11.3 for $\varepsilon = 1.50\%$. Therefore, our results show that the superconducting anisotropy is sensitive to the applied biaxial strain. In addition, for the two levels of tensile strain, γ shows clear enhancement with temperature at around $t = 0.5$, with the enhancement persists to $t \rightarrow 1$ for $\varepsilon = 1.50\%$, but not for $\varepsilon = 1.15\%$. Such a difference may be related to the difference in the dimensionality of the superconductivity. For example, γ diverges when $t \rightarrow 1$ for

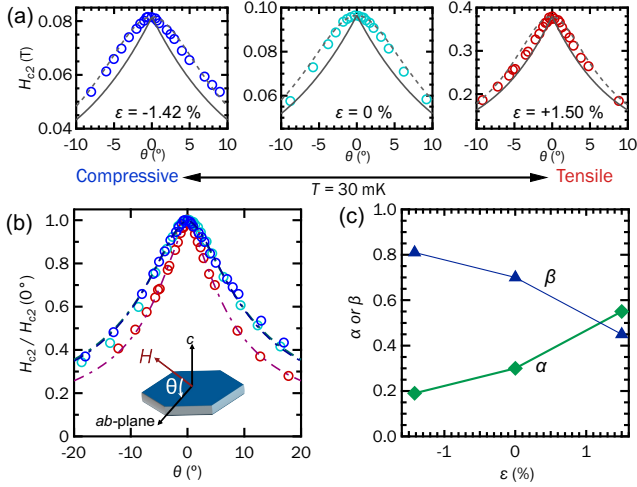


FIG. 4. (a) Angular dependence of upper critical field ($H_{c2}(\theta)$) near $\theta = 0^\circ$ with different strains at 30 mK, the solid line represents the simulated $H_{c2}(\theta)$ by Tinkham model while the dash gray line represents the simulated $H_{c2}(\theta)$ by Ginzburg-Landau anisotropic mass model. (b) Normalized $H_{c2}(\theta)$ near $\theta = 0^\circ$ with different strains at 30 mK, fitted with Eqn. 1. (c) The fitting coefficients α and β as the function of strain.

2D superconductivity⁴⁸. The differences in the magnitudes of γ for two tensile-strained RbV_3Sb_5 samples and their distinct responses to temperature suggest that the superconducting dimensionality and the enhancement of T_c under tensile strain may be correlated.

To get a deeper understanding, we directly probe the superconducting dimensionality by measuring the angular dependence of the upper critical field ($H_{c2}(\theta)$). The schematic of the sample orientation and field direction is shown in the inset of Fig. 4(b). Figure 4(a) shows the $H_{c2}(\theta)$ under different levels of strain at 30 mK. Here, we use the anisotropic mass Ginzburg-Landau model (GL model) and the Tinkham model⁴⁸, which are commonly employed to describe 3D and 2D superconductivity, respectively. Their major difference is that, $H_{c2}(\theta)$ is smooth for all θ in the GL model, but a cusp appears at $\theta = 0^\circ$ in the Tinkham model. We simulate $H_{c2}(\theta)$ using both the GL model and the Tinkham model for the three cases shown in Fig. 4(a) and present them as dotted line and solid line, respectively. For these simulations, we have used the experimental $H_{c2}(0^\circ)$ and $H_{c2}(90^\circ)$ at respective strains as input parameters. For the compressive strain ($\epsilon = -1.42\%$) and free-standing ($\epsilon = 0\%$) cases, $H_{c2}(\theta)$ displays a smooth maximum across $\theta = 0^\circ$, and the datasets are better described by the GL model. For the tensile strain case, the $H_{c2}(\theta)$ exhibits a sharper maximum across $\theta = 0^\circ$, and the dataset falls between the simulations by the GL and Tinkham model. Therefore, the simulations imply a change in dimensionality of the superconductivity in RbV_3Sb_5 under tensile strain. To better fit the dataset and quantify the contribution of 2D and 3D superconductivity involved in the $H_{c2}(\theta)$ of RbV_3Sb_5 under different levels of strain, we adopt the combination of GL model and Tinkham model^{49–52}, which have the following

form:

$$\left[\frac{H_{c2}(\theta) \cos \theta}{H_{c2}(0^\circ)} \right]^2 + \alpha \left| \frac{H_{c2}(\theta) \sin \theta}{H_{c2}(90^\circ)} \right| + \beta \left[\frac{H_{c2}(\theta) \sin \theta}{H_{c2}(90^\circ)} \right]^2 = 1 \quad (1)$$

where α and β are the fitting parameters that quantify how closely $H_{c2}(\theta)$ resembles the Tinkham model and the GL model respectively. We anticipate the sum of α and β to be 1, and this is confirmed by our fitting results. Figure 4(b) shows the fits of normalized $H_{c2}(\theta)$ at the different levels of strain to the combined model. All the datasets can be well described by the combined model. The extracted α and β for different strain values are shown in Fig. 4(c). For the free-standing case, α is 0.30, which indicates a larger contribution of 3D superconductivity. Upon applying a compressive strain, the α is 0.19, indicating that the 2D character is suppressed, approaching the GL model (3D) limit. On the other hand, with tensile strain, α increases to 0.55, indicating a shift in the dimensionality towards the 2D side. Interestingly, under the free-standing condition, CsV_3Sb_5 already exhibits 2D superconductivity⁵³, and its T_c is higher than that of RbV_3Sb_5 . Since the T_c enhancement in RbV_3Sb_5 is accompanied by the shift in the dimensionality of the superconductivity from predominantly 3D to a more 2D character, the results suggests that 2D superconductivity plays an important role in the T_c enhancement in the AV_3Sb_5 family.

While hydrostatic pressure has previously been employed to enhance T_c of RbV_3Sb_5 ³⁹, the present study provides a different yet complementary avenue for tuning the superconductivity in RbV_3Sb_5 . We argue that the methodology used herein has several distinct advantages. First, hydrostatic pressure is inherently compressive, whereas biaxial strain can be either compressive or tensile in the planar direction. This unique property of biaxial strain allows for greater flexibility in tuning. The fact that only two spatial directions are actively modified further enables us to conclude that the c -axis length serves as the decisive tuning parameter for T_c in RbV_3Sb_5 . Second, the biaxial device offers an excellent platform for optical measurements, because the sample is not obstructed, unlike the case of hydrostatic pressure where the optical path is limited by the materials surrounding the samples. Thus, the investigation of strained RbV_3Sb_5 with optical methods can be suitable for further projects.

The shift towards a superconducting state with a more 2D character could be due to a more 2D-like Fermi surface under tensile strain. This trend might be counterintuitive, but it is possible that the electronic structure has been modified in such a way that some 3D Fermi pockets disappear when the c -axis is shorter, which happens when an in-plane tensile biaxial strain is applied. This would allow the 2D character to dominate, as reflected in the dimensionality of superconductivity. This unusual behavior has been reported in MoTe_2 , where the Fermi surface becomes more 2D-like under pressure⁵⁴. Furthermore, a Lifshitz transition can be associated with the disappearance of 3D pockets, which could explain the observed jump in $\Delta T_c/T_c$ displayed in Fig. 1(b). Quantum oscillation data against the field angle can probe the dimensionality of the Fermi surface. The current design is compatible with such a measurement, allowing the discussion of both

the superconducting and the normal state anisotropies by conducting measurements in strong magnetic fields. Recently, we demonstrated the measurement of quantum oscillations up to 60 T in a pulsed magnet¹³. Thus, we do not anticipate significant barriers in measuring quantum oscillations in biaxially strained RbV₃Sb₅ against the field angle.

To summarize, we have studied the biaxial strain effect on the superconductivity in RbV₃Sb₅, using substrates with different thermal expansion coefficients. In particular, T_c is enhanced drastically from 0.82 K to 1.46 K with the maximum tensile strain ($\varepsilon = 1.50\%$) exerted by the negative thermal expansion substrate ZrW₂O₈. We further examine the temperature dependence of H_{c2} in tensile strained RbV₃Sb₅. Multi-band behavior is inferred for $\varepsilon = 1.15\%$, while single-band behavior arises for $\varepsilon = 1.50\%$. The significant increase in the extracted anisotropy factor γ suggests the correlation between T_c enhancement and the shift in the superconducting dimensionality. This shift is quantified by the model that combines the Tinkham model and the anisotropic mass Ginzburg-Landau model, showing the shift towards 2D superconductivity. Our work consolidates the biaxial strain as a promising tool to tune quasi-2D materials, and paves the way for the understanding of the superconductivity in AV₃Sb₅ family.

SUPPLEMENTARY MATERIAL

The X-ray diffraction pattern of ZrW₂O₈, nominal strain induced on RbV₃Sb₅ by substrates, and extraction of isotropic response $\varepsilon_{A_{1g}}$ from uniaxial strain experiment are described in the Supplementary Material.

ACKNOWLEDGMENTS

[§]T. F. Poon and K. Y. Yip contributed equally to this work. The work was supported by the Research Grants Council of Hong Kong (Grant Nos. A-CUHK 402/19, CUHK 14301020, CUHK 14300722, CUHK 14302724), CUHK Direct Grant (4053577, 4053664), and the Guangdong Provincial Quantum Science Strategic Initiative (Grant No. GDZX2301009).

AUTHOR DECLARATIONS

Conflict of Interest

The authors have no conflicts to disclose.

DATA AVAILABILITY STATEMENT

The data that support the findings of this study are available from the corresponding author upon reasonable request.

¹H. Takahashi, K. Igawa, K. Arii, Y. Kamihara, M. Hirano, and H. Hosono, "Superconductivity at 43 K in an iron-based layered compound LaO_{1-x}F_xFeAs," *Nature* **453**, 376 (2008).

- ²H. Kotegawa, H. Sugawara, and H. Tou, "Abrupt emergence of pressure-induced superconductivity of 34 K in SrFe₂As₂: A resistivity study under pressure," *Phys. Soc. Jpn.* **78**, 013709 (2009).
- ³P. L. Alireza, Y. C. Ko, J. Gillett, C. M. Petrone, J. M. Cole, G. G. Lonzarich, and S. E. Sebastian, "Superconductivity up to 29 K in SrFe₂As₂ and BaFe₂As₂ at high pressures," *J. Condens. Matter Phys.* **21**, 012208 (2008).
- ⁴S. K. Goh, Y. Nakai, K. Ishida, L. Klintberg, Y. Ihara, S. Kasahara, T. Shibauchi, Y. Matsuda, and T. Terashima, "Anisotropic superconducting properties of optimally doped BaFe₂(As_{0.65}P_{0.35})₂ under pressure," *Phys. Rev. B* **82**, 094502 (2010).
- ⁵K. Yip, Y. Chan, Q. Niu, K. Matsuura, Y. Mizukami, S. Kasahara, Y. Matsuda, T. Shibauchi, and S. K. Goh, "Weakening of the diamagnetic shielding in FeSe_{1-x}S_x at high pressures," *Phys. Rev. B* **96**, 020502(R) (2017).
- ⁶J. Markert, E. Early, T. Bjørnholm, S. Ghamaty, B. Lee, J. Neumeier, R. Price, C. Seaman, and M. Maple, "Two new electron cuprate superconductors, Pr_{1.85}Th_{0.15}CuO_{4-y} and Eu_{1.85}Ce_{0.15}CuO_{4-y}, and properties of Nd_{2-x}Ce_xO_{4-y}," *Physica C* **158**, 178 (1989).
- ⁷L. Gao, Y. Xue, F. Chen, Q. Xiong, R. Meng, D. Ramirez, C. Chu, J. Eggert, and H. Mao, "Superconductivity up to 164 K in HgBa₂Ca_{m-1}Cu_mO_{2m+2+δ} ($m = 1, 2$, and 3) under quasihydrostatic pressures," *Phys. Rev. B* **50**, 4260(R) (1994).
- ⁸D. Goldschmidt, A.-K. Klehe, J. Schilling, and Y. Eckstein, "Pressure dependence of T_c in cuprate superconductors: Application to (Ca₁La_{1-x})(Ba_{1.75-x}La_{0.25+x})Cu₃O_y," *Phys. Rev. B* **53**, 14631 (1996).
- ⁹M. Monteverde, C. Acha, M. Núñez-Regueiro, D. Pavlov, K. Lokshin, S. Putilin, and E. Antipov, "High-pressure effects in fluorinated HgBa₂Ca₂Cu₃O_{8+δ}," *Europhys. Lett.* **72**, 458 (2005).
- ¹⁰M. Nakajima, Y. Ohata, and S. Tajima, "Control of band structure of FeSe single crystals via biaxial strain," *Phys. Rev. Mater.* **5**, 044801 (2021).
- ¹¹A. E. Böhrer, A. Sapkota, A. Kreyssig, S. L. Bud'ko, G. Drachuck, S. Saunders, A. Goldman, and P. Canfield, "Effect of biaxial strain on the phase transitions of Ca(Fe_{1-x}Co_x)₂As₂," *Phys. Rev. Lett.* **118**, 107002 (2017).
- ¹²K. Y. Yip, S. T. Lam, K. H. Yu, W. S. Chow, J. Zeng, K. T. Lai, and S. K. Goh, "Drastic enhancement of the superconducting temperature in type-II Weyl semimetal candidate MoTe₂ via biaxial strain," *APL Mater.* **11**, 021111 (2023).
- ¹³K. Y. Yip, L. Wang, T. F. Poon, K. H. Yu, S. T. Lam, K. T. Lai, J. Singleton, F. F. Balakirev, and S. K. Goh, "Shubnikov-de Haas oscillations of biaxial-strain-tuned superconductors in pulsed magnetic field up to 60 T," *APL Mater.* **12**, 021124 (2024).
- ¹⁴B. R. Ortiz, L. C. Gomes, J. R. Morey, M. Winiarski, M. Bordelon, J. S. Mangum, I. W. H. Oswald, J. A. Rodriguez-Rivera, J. R. Neilson, S. D. Wilson, E. Ertekin, T. M. McQueen, and E. S. Toberer, "New kagome prototype materials: discovery of KV₃Sb₅, RbV₃Sb₅, and CsV₃Sb₅," *Phys. Rev. Mater.* **3**, 094407 (2019).
- ¹⁵B. R. Ortiz, S. M. L. Teicher, Y. Hu, J. L. Zuo, P. M. Sarte, E. C. Schueller, A. M. M. Abeykoon, M. J. Krogstad, S. Rosenkranz, R. Osborn, R. Seshadri, L. Balents, J. He, and S. D. Wilson, "CsV₃Sb₅: A \mathbb{Z}_2 Topological Kagome Metal with a Superconducting Ground State," *Phys. Rev. Lett.* **125**, 247002 (2020).
- ¹⁶T. Neupert, M. M. Denner, J.-X. Yin, R. Thomale, and M. Z. Hasan, "Charge order and superconductivity in kagome materials," *Nat. Phys.* **18**, 137 (2022).
- ¹⁷H. Li, T. T. Zhang, T. Yilmaz, Y. Y. Pai, C. E. Marvinney, A. Said, Q. W. Yin, C. S. Gong, Z. J. Tu, E. Vescovo, C. S. Nelson, R. G. Moore, S. Murakami, H. C. Lei, H. N. Lee, B. J. Lawrie, and H. Miao, "Observation of Unconventional Charge Density Wave without Acoustic Phonon Anomaly in Kagome Superconductors AV₃Sb₅ ($A = \text{Rb, Cs}$)," *Phys. Rev. X* **11**, 031050 (2021).
- ¹⁸Z. Jiang, H. Ma, W. Xia, Z. Liu, Q. Xiao, Z. Liu, Y. Yang, J. Ding, Z. Huang, J. Liu, Y. Qiao, J. Liu, Y. Peng, S. Cho, Y. Guo, J. Liu, and D. Shen, "Observation of Electronic Nematicity Driven by the Three-Dimensional Charge Density Wave in Kagome Lattice KV₃Sb₅," *Nano Lett.* **23**, 5625 (2023).
- ¹⁹J.-X. Yin, B. Lian, and M. Z. Hasan, "Topological kagome magnets and superconductors," *Nature* **612**, 647 (2022).
- ²⁰K. Y. Chen, N. N. Wang, Q. W. Yin, Y. H. Gu, K. Jiang, Z. J. Tu, C. S. Gong, Y. Uwatoko, J. P. Sun, H. C. Lei, J. P. Hu, and J.-G. Cheng, "Double Superconducting Dome and Triple Enhancement of T_c in the Kagome Superconductor CsV₃Sb₅ under High Pressure," *Phys. Rev. Lett.* **126**, 247001 (2021).

- (2021).
- ²¹H. Zhao, H. Li, B. R. Ortiz, S. M. Teicher, T. Park, M. Ye, Z. Wang, L. Balents, S. D. Wilson, and I. Zeljkovic, "Cascade of correlated electron states in the kagome superconductor CsV_3Sb_5 ," *Nature* **599**, 216 (2021).
 - ²²F. H. Yu, T. Wu, Z. Y. Wang, B. Lei, W. Z. Zhuo, J. J. Ying, and X. H. Chen, "Concurrence of anomalous Hall effect and charge density wave in a superconducting topological kagome metal," *Phys. Rev. B* **104**, L041103 (2021).
 - ²³F. Yu, D. Ma, W. Zhuo, S. Liu, X. Wen, B. Lei, J. Ying, and X. Chen, "Unusual competition of superconductivity and charge-density-wave state in a compressed topological kagome metal," *Nat. Commun.* **12**, 3645 (2021).
 - ²⁴Q. Wang, P. Kong, W. Shi, C. Pei, C. Wen, L. Gao, Y. Zhao, Q. Yin, Y. Wu, G. Li, H. Lei, J. Li, Y. Chen, S. Yan, and Y. Qi, "Charge Density Wave Orders and Enhanced Superconductivity under Pressure in the Kagome Metal CsV_3Sb_5 ," *Adv. Mater.* **33**, 2102813 (2021).
 - ²⁵S. Han, C. S. Tang, L. Li, Y. Liu, H. Liu, J. Gou, J. Wu, D. Zhou, P. Yang, C. Diao, J. Ji, J. Bao, L. Zhang, M. Zhao, M. V. Milošević, Y. Guo, L. Tian, M. B. H. Breese, G. Cao, C. Cai, A. T. S. Wee, and X. Yin, "Orbital-Hybridization-Driven Charge Density Wave Transition in CsV_3Sb_5 Kagome Superconductor," *Adv. Mater.* **35**, 2209010 (2023).
 - ²⁶M. Kang, S. Fang, J. Yoo, B. R. Ortiz, Y. M. Oey, J. Choi, S. H. Ryu, J. Kim, C. Jozwiak, A. Bostwick, E. Rotenberg, E. Kaxiras, J. G. Checkelsky, S. D. Wilson, J.-H. Park, and R. Comin, "Charge order landscape and competition with superconductivity in kagome metals," *Nat. Mater.* **22**, 186 (2023).
 - ²⁷W. Zhang, X. Liu, L. Wang, C. W. Tsang, Z. Wang, S. T. Lam, W. Wang, J. Xie, X. Zhou, Y. Zhao, S. Wang, J. Tallon, K. T. Lai, and S. K. Goh, "Nodeless Superconductivity in Kagome Metal CsV_3Sb_5 with and without Time Reversal Symmetry Breaking," *Nano Lett.* **23**, 872 (2023).
 - ²⁸W. Zhang, T. F. Poon, C. W. Tsang, W. Wang, X. Liu, J. Xie, S. T. Lam, S. Wang, K. T. Lai, A. Pourret, G. Seyfarth, G. Knebel, W. C. Yu, and S. K. Goh, "Large Fermi surface in pristine kagome metal CsV_3Sb_5 and enhanced quasiparticle effective masses," *Proc. Natl. Acad. Sci. USA* **121**, e2322270121 (2024).
 - ²⁹F. Du, S. Luo, B. R. Ortiz, Y. Chen, W. Duan, D. Zhang, X. Lu, S. D. Wilson, Y. Song, and H. Yuan, "Pressure-induced double superconducting domes and charge instability in the kagome metal KV_3Sb_5 ," *Phys. Rev. B* **103**, L220504 (2021).
 - ³⁰S.-Y. Yang, Y. Wang, B. R. Ortiz, D. Liu, J. Gayles, E. Derunova, R. Gonzalez-Hernandez, L. Šmejkal, Y. Chen, S. S. P. Parkin, S. D. Wilson, E. S. Toberer, T. McQueen, and M. N. Ali, "Giant, unconventional anomalous Hall effect in the metallic frustrated magnet candidate, KV_3Sb_5 ," *Sci. Adv.* **6**, eabb6003 (2020).
 - ³¹H. Luo, Q. Gao, H. Liu, Y. Gu, D. Wu, C. Yi, J. Jia, S. Wu, X. Luo, Y. Xu, L. Zhao, Q. Wang, H. Mao, G. Liu, Z. Zhu, Y. Shi, K. Jiang, J. Hu, Z. Xu, and X. J. Zhou, "Electronic nature of charge density wave and electron-phonon coupling in kagome superconductor KV_3Sb_5 ," *Nat. Commun.* **13**, 273 (2022).
 - ³²Z. Wang, W. Zhang, L. Wang, T. F. Poon, C. W. Tsang, W. Wang, J. Xie, S. T. Lam, X. Zhou, Y. Zhao, S. Wang, M.-Z. Ai, K. T. Lai, and S. K. Goh, "Similarities and differences in the fermiology of kagome metals AV_3Sb_5 ($A=\text{K}, \text{Rb}, \text{Cs}$) revealed by Shubnikov-de Haas oscillations," *Appl. Phys. Lett.* **123**, 012601 (2023).
 - ³³Z. Wang, L. Wang, K. Y. Yip, Y. K. Tsui, T. F. Poon, W. Wang, C. W. Tsang, S. Wang, D. Graf, A. Pourret, G. Seyfarth, G. Knebel, K. T. Lai, W. C. Yu, W. Zhang, and S. K. Goh, "Discovery of a New Phase in Thin Flakes of KV_3Sb_5 under Pressure," *Adv. Sci.* , 2415012 (2025).
 - ³⁴Z. Guguchia, C. Mielke, D. Das, R. Gupta, J.-X. Yin, H. Liu, Q. Yin, M. H. Christensen, Z. Tu, C. Gong, N. Shumiya, M. S. Hossain, T. Gamsakhurdashvili, M. Elender, P. Dai, A. Amato, Y. Shi, H. C. Lei, R. M. Fernandes, M. Z. Hasan, H. Luetkens, and R. Khasanov, "Tunable unconventional kagome superconductivity in charge ordered RbV_3Sb_5 and KV_3Sb_5 ," *Nat. Commun.* **14**, 153 (2023).
 - ³⁵C. C. Zhu, X. F. Yang, W. Xia, Q. W. Yin, L. S. Wang, C. C. Zhao, D. Z. Dai, C. P. Tu, B. Q. Song, Z. C. Tao, Z. J. Tu, C. S. Gong, H. C. Lei, Y. F. Guo, and S. Y. Li, "Double-dome superconductivity under pressure in the V-based kagome metals AV_3Sb_5 ($A = \text{Rb}$ and K)," *Phys. Rev. B* **105**, 094507 (2022).
 - ³⁶L. Wang, W. Zhang, Z. Wang, T. F. Poon, W. Wang, C. W. Tsang, J. Xie, X. Zhou, Y. Zhao, S. Wang, K. T. Lai, and S. K. Goh, "Anomalous Hall effect and two-dimensional Fermi surfaces in the charge-density-wave state of kagome metal RbV_3Sb_5 ," *J. Phys. Mater.* **6**, 02LT01 (2023).
 - ³⁷Q. Yin, Z. Tu, C. Gong, Y. Fu, S. Yan, and H. Lei, "Superconductivity and Normal-State Properties of Kagome Metal RbV_3Sb_5 Single Crystals," *Chin. Phys. Lett.* **38**, 037403 (2021).
 - ³⁸F. Du, S. Luo, R. Li, B. R. Ortiz, Y. Chen, S. D. Wilson, Y. Song, and H. Yuan, "Evolution of superconductivity and charge order in pressurized RbV_3Sb_5 ," *Chin. Phys. B* **31**, 017404 (2022).
 - ³⁹N. N. Wang, K. Y. Chen, Q. W. Yin, Y. N. N. Ma, B. Y. Pan, X. Yang, X. Y. Ji, S. L. Wu, P. F. Shan, S. X. Xu, Z. J. Tu, C. S. Gong, G. T. Liu, G. Li, Y. Uwatoko, X. L. Dong, H. C. Lei, J. P. Sun, and J.-G. Cheng, "Competition between charge-density-wave and superconductivity in the kagome metal RbV_3Sb_5 ," *Phys. Rev. Res.* **3**, 043018 (2021).
 - ⁴⁰J. Evans, T. Mary, T. Vogt, M. Subramanian, and A. Sleight, "Negative Thermal Expansion in ZrW_2O_8 and HfW_2O_8 ," *Chem. Mater.* **8**, 2809 (1996).
 - ⁴¹L. L. Chang, M. Scroger, and B. Phillips, "Condensed Phase Relations in the Systems $\text{ZrO}_2\text{-WO}_2\text{-WO}_3$ and $\text{HfO}_2\text{-WO}_2\text{-WO}_3$," *J. Am. Ceram. Soc.* **50**, 211 (1967).
 - ⁴²T. Qian, M. H. Christensen, C. Hu, A. Saha, B. M. Andersen, R. M. Fernandes, T. Birol, and N. Ni, "Revealing the competition between charge density wave and superconductivity in CsV_3Sb_5 through uniaxial strain," *Phys. Rev. B* **104**, 144506 (2021).
 - ⁴³S. Stoupin and Y. V. Shvyd'ko, "Thermal Expansion of Diamond at Low Temperatures," *Phys. Rev. Lett.* **104**, 085901 (2010).
 - ⁴⁴X. Yang, Q. Tang, Q. Zhou, H. Wang, Y. Li, X. Fu, J. Zhang, Y. Song, H. Yuan, P. Dai, and X. Lu, "In-plane uniaxial-strain tuning of superconductivity and charge-density wave in CsV_3Sb_5 ," *Chin. Phys. B* **32**, 127101 (2023).
 - ⁴⁵M. Frachet, L. Wang, W. Xia, Y. Guo, M. He, N. Maraytta, R. Heid, A.-A. Haghighirad, M. Merz, C. Meingast, and F. Hardy, "Colossal c -axis response and lack of rotational symmetry breaking within the kagome planes of the CsV_3Sb_5 superconductor," *Phys. Rev. Lett.* **132**, 186001 (2024).
 - ⁴⁶S. Ni, S. Ma, Y. Zhang, J. Yuan, H. Yang, Z. Lu, N. Wang, J. Sun, Z. Zhao, D. Li, S. Liu, H. Zhang, H. Chen, K. Jin, J. Cheng, L. Yu, F. Zhou, X. Dong, J. Hu, H.-J. Gao, and Z. Zhao, "Anisotropic Superconducting Properties of Kagome Metal CsV_3Sb_5 ," *Chin. Phys. Lett.* **38**, 057403 (2021).
 - ⁴⁷N. Werthamer, E. Helfand, and P. Hohenberg, "Temperature and Purity Dependence of the Superconducting Critical Field, H_{c2} . III. Electron Spin and Spin-Orbit Effects," *Phys. Rev.* **147**, 295 (1966).
 - ⁴⁸M. Tinkham, "Effect of Fluxoid Quantization on Transitions of Superconducting Films," *Phys. Rev.* **129**, 2413 (1963).
 - ⁴⁹S. K. Goh, Y. Mizukami, H. Shishido, D. Watanabe, S. Yasumoto, M. Shimozawa, M. Yamashita, T. Terashima, Y. Yanase, T. Shibauchi, A. I. Buzdin, and Y. Matsuda, "Anomalous Upper Critical Field in $\text{CeCoIn}_5/\text{YbCoIn}_5$ Superlattices with a Rashba-Type Heavy Fermion Interface," *Phys. Rev. Lett.* **109**, 157006 (2012).
 - ⁵⁰M. Shimozawa, S. K. Goh, R. Endo, R. Kobayashi, T. Watashige, Y. Mizukami, H. Ikeda, H. Shishido, Y. Yanase, T. Terashima, T. Shibauchi, and Y. Matsuda, "Controllable Rashba Spin-Orbit Interaction in Artificially Engineered Superlattices Involving the Heavy-Fermion Superconductor CeCoIn_5 ," *Phys. Rev. Lett.* **112**, 156404 (2014).
 - ⁵¹M. Uchida, M. Ide, M. Kawamura, K. S. Takahashi, Y. Kozuka, Y. Tokura, and M. Kawasaki, "Anomalous enhancement of upper critical field in Sr_2RuO_4 thin films," *Phys. Rev. B* **99**, 161111(R) (2019).
 - ⁵²L. E. Chow, K. Rubi, K. Y. Yip, M. Pierre, M. Leroux, X. Liu, Z. Luo, S. Zeng, C. Li, M. Goiran, N. Harrison, W. Escoffier, S. K. Goh, and A. Ariando, "Dimensionality control and rotational symmetry breaking superconductivity in square-planar layered nickelates," *arXiv:2301.07606* (2023).
 - ⁵³M. S. Hossain, Q. Zhang, E. S. Choi, D. Ratkovski, B. Lüscher, Y. Li, Y.-X. Jiang, M. Litskevich, Z.-J. Cheng, J.-X. Yin, T. A. Cochran, B. Casas, B. Kim, X. Yang, J. Liu, Y. Yao, A. Bangura, Z. Wang, M. H. Fischer, T. Neupert, L. Balicas, and M. Z. Hasan, "Unconventional gapping behaviour in a kagome superconductor," *Nat. Phys.* **21**, 556 (2025).
 - ⁵⁴Y. J. Hu, W. C. Yu, K. T. Lai, D. Sun, F. F. Balakirev, W. Zhang, J. Y. Xie, K. Y. Yip, E. I. P. Aulestia, R. Jha, R. Higashinaka, T. D. Matsuda, Y. Yanase, Y. Aoki, and S. K. Goh, "Detection of Hole Pockets in the Candidate Type-II Weyl Semimetal MoTe_2 from Shubnikov-de Haas Quantum Oscillations," *Phys. Rev. Lett.* **124**, 076402 (2020).